

# PROCEEDINGS OF SPIE

[SPIDigitalLibrary.org/conference-proceedings-of-spie](https://SPIDigitalLibrary.org/conference-proceedings-of-spie)

## 300mm in-line metrologies for the characterization of ultra-thin layer of 2D materials

A. Moussa, J. Bogdanowicz, B. Groven, P. Morin, M. Beggiato, et al.

A. Moussa, J. Bogdanowicz, B. Groven, P. Morin, M. Beggiato, M. Saib, G. Santoro, Y. Abramovitz, K. Houtchens, S. Ben Nissim, N. Meir, J. Hung, A. Urbanowicz, R. Koret, I. Turovets, G. F. Lorusso, A.-L. Charley, "300mm in-line metrologies for the characterization of ultra-thin layer of 2D materials," Proc. SPIE 12496, Metrology, Inspection, and Process Control XXXVII, 124961X (27 April 2023); doi: 10.1117/12.2657968

**SPIE.**

Event: SPIE Advanced Lithography + Patterning, 2023, San Jose, California, United States

# 300mm in-line metrologies for the characterization of ultra-thin layer of 2D materials

A. Moussa<sup>a</sup>, J. Bogdanowicz<sup>a</sup>, B. Groven<sup>a</sup>, P. Morin<sup>a</sup>, M. Beggiato<sup>a</sup>, M. Saib<sup>a</sup>, G. Santoro<sup>b</sup>, Y. Abramovitz<sup>c</sup>, K. Houchens<sup>c</sup>, S. Ben Nissim<sup>c</sup>, N. Meir<sup>d</sup>, J. Hung<sup>d</sup>, A. Urbanowicz<sup>d</sup>, R. Koret<sup>d</sup>, I. Turovets<sup>d</sup>, G. F. Lorusso<sup>a</sup>, A.-L. Charley<sup>a</sup>

<sup>a</sup> imec, 3001 Leuven, Belgium

<sup>b</sup> Applied Materials, 3001 Leuven, Belgium

<sup>c</sup> Applied Materials, Rehovot, Israel

<sup>d</sup> NOVA, Rehovot 7632805, Israel

## ABSTRACT

Devices based on 2D material channels require high-quality monolayer material. However, although the value of many laboratory metrology techniques has been demonstrated on small coupons, the development of inline characterization of 2D material layers grown on full 300mm wafers is still missing. In this work, we evaluate and combine different inline metrologies to characterize at wafer level the thickness and the morphology of tungsten disulfide (WS<sub>2</sub>) layers grown on full 300mm wafers. Combining the results from the different techniques allows us to reveal the morphology and the thickness of the WS<sub>2</sub> layers as well as their uniformity across the 300 mm wafers for different growth conditions.

**Keywords:** 2D material, WS<sub>2</sub>, Tungsten disulfide, in-line metrology, 300mm wafer.

## 1-INTRODUCTION

The next extension of Moore's law will occur through a multitude of approaches. Beyond the traditional scaling and the new 3D device architectures, the roadmap also foresees a transition from Si to new atomic layer channel [1]. Such devices based on 2D material channels require high-quality monolayer material. Indeed, the control of the thickness and the crystallinity of the layer will define its physical properties. However, the development of inline characterization of 2D material layers grown on full 300mm wafers is still missing.

In this work, we evaluate and combine different inline metrologies to characterize at wafer level the thickness and the morphology of tungsten disulfide (WS<sub>2</sub>) layers grown on 300mm wafers. We used a set of 4 wafers with different deposition conditions resulting in wafers with 0 to 2 monolayers with varying layer coverages from a non-closed layer to multilayers. These wafers were characterized using 4 in-line techniques. First, atomic force microscopy (AFM) provides the topography of the layer, its roughness, and the layer step-height. Second, scanning electron microscopy (SEM) reveals the coverage of the different layer thicknesses via their contrast in the SEM images. Finally, optical metrologies like scatterometry and Raman provide information about the averaged thickness of the layer and about its morphology. Combining the results from the 4 techniques reveals the morphology and the thickness of the WS<sub>2</sub> layers as well as their uniformity across the 300 mm wafers for different growth conditions.

## 2- EXPERIMENTAL

Due to the very thin structure of WS<sub>2</sub>, metrology remains difficult. Indeed, a monolayer of WS<sub>2</sub> has a thickness of less than one nanometre. Given the atomic resolution in the Z direction of AFM, this is our first candidate for measuring the topography and the thickness of the layer. However, as we want to characterize the layer across the 300mm wafer, the AFM throughput remains too low to perform it in a decent time. Scanning Electron Microscopy has been dedicated to

managing throughput and characterizing the layer coverage and uniformity on the wafer. The two last techniques evaluated in this work are optical metrology, scatterometry (OCD) and Raman analysis. They provide information about the thickness and the morphology of the layer.

### 2.1-Atomic Force Microscopy.

AFM is a Scanning Probe Microscopy (SPM), the measurement is performed directly by recording the deflection of a laser spot reflected on a probe scanning on top of the sample, this set up has atomic resolution in Z direction. In this work, the measurements were performed with Park Systems NX3DM tool, in “true non-contact” mode, which causes less damage to the sample and increases the probe lifetime. As the throughput of AFM is low, only 6 measurements of  $1 \times 1 \mu\text{m}^2$ , were made per wafer, from the centre to the edge of the wafer. Each image was flattened with a first-order regression. The histogram analysis of the images provides the topography and the thickness of the layer.

### 2.2-Scanning Electron Microscopy.

The SEM analysis of the layer across the wafer has been realised with a tool from Applied Materials. Acquisition conditions have been tuned to optimise the contrast between substrate, the monolayer, and the multi-layer of  $\text{WS}_2$ . Thanks to the throughput of the tool, 89 images of  $1 \times 1 \mu\text{m}^2$  were acquired across each wafer. The analysis of the images provides the coverage area of the substrate, the monolayer, and the multi-layer of  $\text{WS}_2$  in each image.

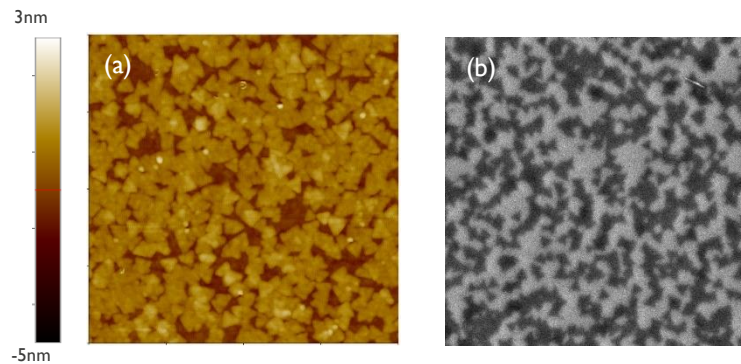


Figure 1: image of  $1 \times 1 \mu\text{m}^2$  (a) from AFM with the z-scale on the right, (b) from SEM.

### 2.3-Scatterometry.

Scatterometry is an optical model-based technique suitable for the characterization of the layer thickness [2]. Same wafer-map than SEM has been used for the analysis across the wafer with a shift to avoid possible damages from other technique. The Nova MMSR scatterometry tool used in this work exploits a wide range of wavelengths at multiple azimuths and angles of incidence. The reconstruction of the spectrum via model provides the thickness of the  $\text{WS}_2$  layer averaged over the spot area. Figure 2a shows the spectrum from the reference sample and sample with a monolayer (A), this reveals the sensitivity of the scatterometry.

### 2.4-Raman analysis.

Raman spectrums were acquired on the Nova ELIPSON<sup>TM</sup> tool. This analysis has been done on each wafer with 45-points wafer map. As described in literature [3], the position and intensity of the  $E_{2g}$  and  $A_{1g}$  peaks in the Raman spectrum provide information about the layer thickness and morphology across the wafer. Like most optical metrology, the signal is averaged over the spot area.

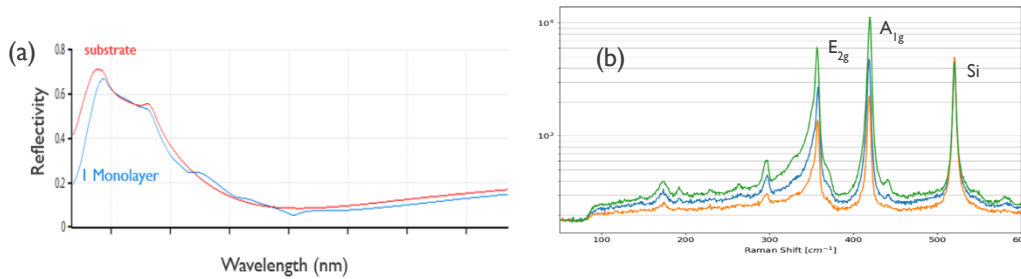


Figure 2: (a) Scatterometry spectrum for substrate (red) and one monolayer of WS<sub>2</sub> on substrate (Blue), (b) Raman spectrum for layer of WS<sub>2</sub> with different thicknesses.

### 3-RESULTS AND DISCUSSION

In this section, we show and discuss the results of each metrology on a set of 4 samples. This set consists of one sample (A) with POR growth for monolayer thickness, two samples (B and C) where the WS<sub>2</sub> layer has different thickness and coverage across the sample, and finally one sample (D) with large and isolated islands of WS<sub>2</sub>. The combination and the correlation of the results of the different metrologies make it possible to describe the layer of 2D material for each sample.

#### 3.1-AFM and SEM.

AFM provides true height distribution of the layer while SEM provides grayscale contrast of the layer. The AFM image and the SEM image of the same isolated island (D) allow us to attribute the different contrast in the SEM image to the layer thickness in the AFM image (Fig. 3).

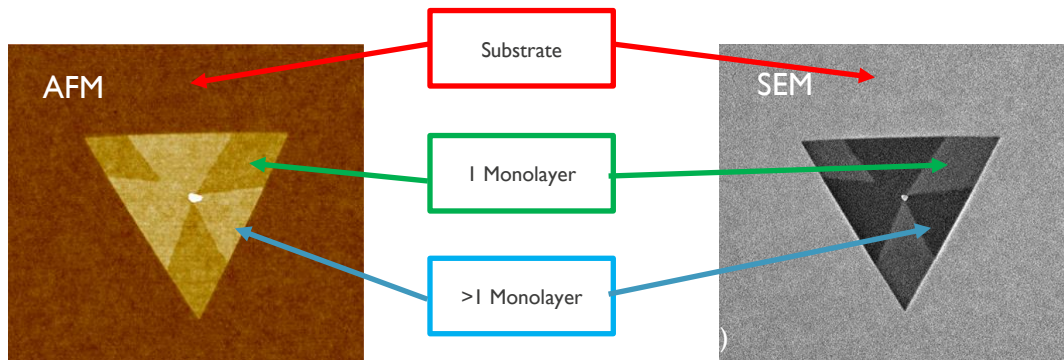


Figure 3: 4x4 μm<sup>2</sup> image of an isolated island of WS<sub>2</sub> (a) from AFM, (b) from SEM

Therefore, the peaks in the histogram analysis of AFM and SEM images (Fig. 1) can be attributed to substrate, monolayer, and multiple monolayer thicknesses. Figure 4 shows the histogram analysis of each sample for AFM and SEM images. the coloured boxes show the range of height and grayscale assigned to the different layer thicknesses, red: substrate, green: monolayer and blue: more than monolayer.

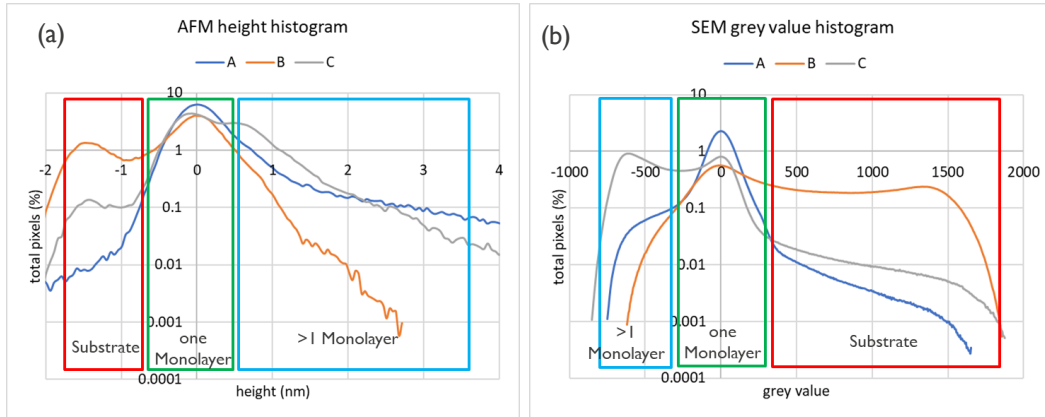


Figure 4: Histogram overlay for an image of sample A, B and C (a) from AFM, (b) from SEM, note: the histograms are aligned to the peak assigned to the monolayer.

Histogram analysis from SEM images allows us to create wafer coverage maps for each height range or plot it against wafer radius (Fig. 5). Figure 5 shows the layer uniformity for sample A when it shows a radial trend for Samples B and C. This is because Sample B has mostly a monolayer with less coverage in the centre than near the edge and sample C has the same trend but starting, mostly, from a single layer in the centre to a multi-layer near the edge.

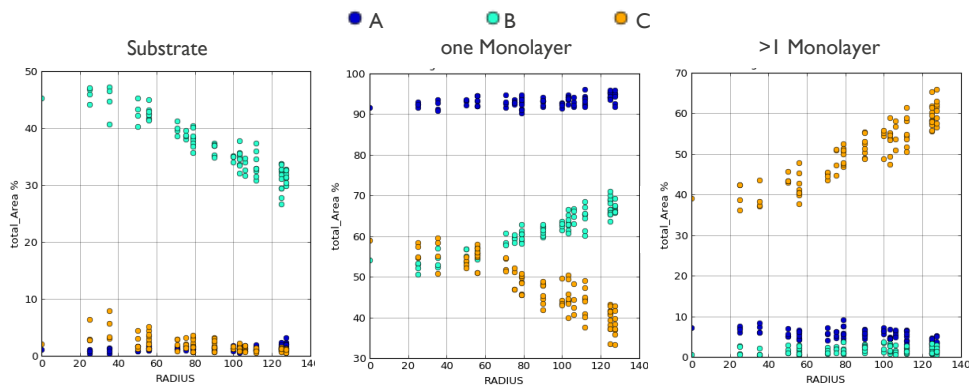


Figure 5: Percentage coverage per step height for samples A, B and C versus the wafer radius left: Substrate, centre: one monolayer, right: more than one monolayer,

### 3.2-Scatterometry.

As mentioned in 2.3, Scatterometry provides the average thickness of the layer of  $WS_2$  in the spot area. Figure 6 shows the result, as wafer map, for the samples A, B and C. For each sample a radial trend is visible but if sample A has a thicker layer in the centre, Sample B and C show the opposite. Furthermore, sample A is more homogenous than B and C.

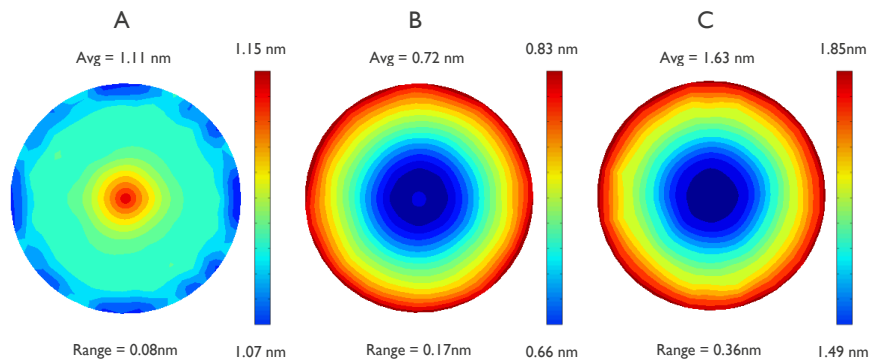


Figure 6: Results from scatterometry, average thickness of the layer of WS<sub>2</sub>, respectively from left to right for sample A, B and C

These results can be compared with the results of the SEM image analysis. Indeed, in the SEM image, the amount of WS<sub>2</sub> can be evaluated by the sum of the coverage of the monolayer and two times the coverage of the multilayer. Figure 7 shows this correlation, the correlation coefficient between this calculation and the result of the scatterometry is equal to 0.9981, which confirms us that the 2-dimensions analysis of the SEM image agrees with the average thickness measured via scatterometry.

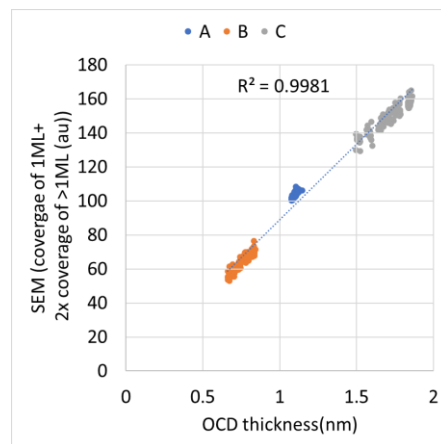


Figure 7: correlation between scatterometry results and SEM image analysis, for sample A, B and C. The correlation coefficient was calculated on all the data.

### 3.3-Raman analysis.

As mentioned in 2.4., the intensity and position of the peaks E<sub>2g</sub>, A<sub>1g</sub> and Si in the Raman spectrum provide information about the layer. Figure 8 shows the boxplot for the intensity and the position of these peaks for all measurements per sample. The intensity of the peaks correlates with the thickness of the WS<sub>2</sub> layer. Indeed, the intensity of the E<sub>2g</sub> and A<sub>1g</sub> peaks increases with the thickness when the intensity of the Si peak decreases. This decrease can be explained by the shielding of the substrate by the WS<sub>2</sub> layer when its thickness increases. Also, whatever the thickness of the WS<sub>2</sub> layer, the position of the Si peak is not affected but the positions of the A<sub>1g</sub> and E<sub>2g</sub> peaks are affected. In fact, the position of the A<sub>1g</sub> peak increases with the number of layers. This is explained by the fact that samples A and B mainly have a monolayer of WS<sub>2</sub> and sample C mainly a bilayer. On the contrary, the position of the E<sub>2g</sub> peak decreases with the type of process and the number of layers. As described in literature [4], the difference of the E<sub>2g</sub> peak position for the samples with a monolayer can be explain by a difference in strain in the layer due to the deposition process.

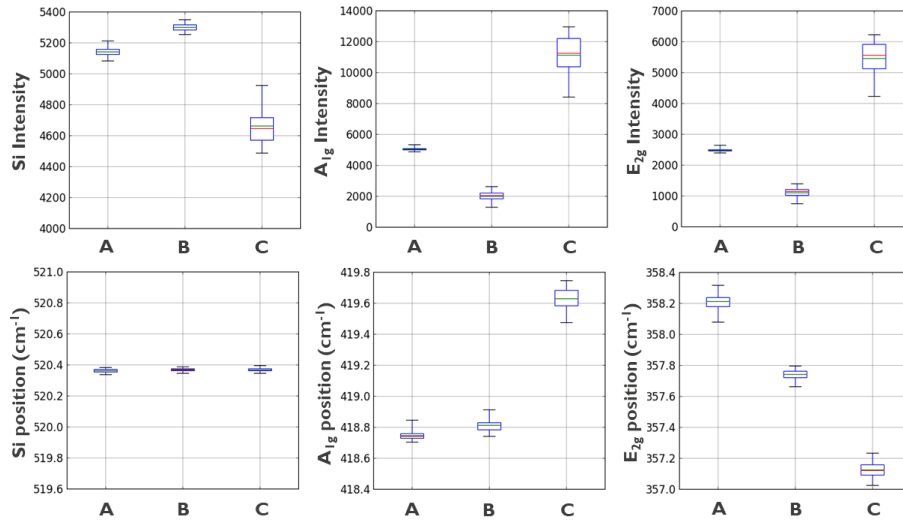


Figure 8: Box plots of, intensity (top) and position (bottom) of the peak of Si, A<sub>1g</sub> and E<sub>2g</sub> with 45 points per sample.

To demonstrate the correlation between the thickness of the layer and the intensity of the peaks A<sub>1g</sub> and E<sub>2g</sub>, Figure 9 shows the correlation plot between the thickness of the WS<sub>2</sub> layer obtain by scatterometry and the intensity of the peak collected on the same site for the three samples. A correlation coefficient higher than 0.99 confirms that the intensity of the A<sub>1g</sub> and E<sub>2g</sub> peaks correspond to the amount of WS<sub>2</sub>.

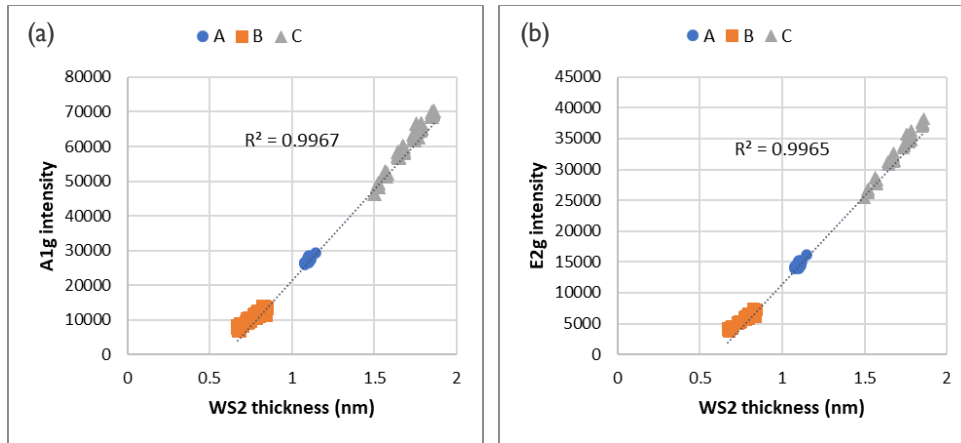


Figure 9: Correlation between WS<sub>2</sub> layer thickness obtain via scatterometry and the intensity of the peaks (a) A<sub>1g</sub> and (b) E<sub>2g</sub> from Raman Spectrum

## 4-SUMMARY AND CONCLUSIONS

In this work, we have evaluated and demonstrated that the combination of different in-line metrologies make it possible to characterize, at wafer level, the thickness and morphology of a layer of WS<sub>2</sub>. First, we showed that AFM can provide the layer thickness and topography. Moreover, combined with SEM, this analysis can be extended, in a decent time, within the wafer coverage. Second, Scatterometry, a fast metrology based on the optical model, can provide full wafer maps of the layer's average thickness. There is an excellent correlation of scatterometry measured average thickness with the thickness calculated based on SEM coverage. Third, Raman optical metrology analysis showed that the intensities of the A<sub>1g</sub> and E<sub>2g</sub> peaks correlate to the layer's average thickness. In addition, the position of these peaks provides information on the morphology of the layer: the shift of the A<sub>1g</sub> peak reveals the presence of a multilayer, and the shift in the E<sub>2g</sub> peak shows the effect of the process on the strain in the layer.

## REFERENCES

- [1] Luc Van den Hove, "The endless progression of Moore's law", Proc. SPIE PC12053, Metrology, Inspection, and Process Control XXXVI; PC120530 (2022).
- [2] Hsiang-Lin Liu and al, "Optical properties of monolayer transition metal dichalcogenides probed by spectroscopic ellipsometry", Applied Physics Letters 105, 201905 (2014).
- [3] Liangbo Liang and al, "First-principles Raman spectra of MoS<sub>2</sub>, WS<sub>2</sub> and their heterostructures", Nanoscale, 2014, 6, 5394
- [4] Fang Wang and al, "Strain-induced phonon shifts in tungsten disulfide nanoplatelets and nanotubes", 2D Mater. 4 (2016) 015007